National Library
of Canada

Acquisitions and
Bibliographic Services Branch

395 Wellington Street
Ottawa, Ontario
K1A 0N4

Bibliothèque nationale
du Canada

Direction des acquisitions et
des services bibliographiques

395, rue Wellington
Ottawa (Ontario)
K1A 0N4

*Your file Votre référence*

*Our file Notre référence*

## NOTICE

The quality of this microform is heavily dependent upon the quality of the original thesis submitted for microfilming. Every effort has been made to ensure the highest quality of reproduction possible.

If pages are missing, contact the university which granted the degree.

Some pages may have indistinct print especially if the original pages were typed with a poor typewriter ribbon or if the university sent us an inferior photocopy.

Reproduction in full or in part of this microform is governed by the Canadian Copyright Act, R.S.C. 1970, c. C-30, and subsequent amendments.

## AVIS

La qualité de cette microforme dépend grandement de la qualité de la thèse soumise au microfilmage. Nous avons tout fait pour assurer une qualité supérieure de reproduction.

S'il manque des pages, veuillez communiquer avec l'université qui a conféré le grade.

La qualité d'impression de certaines pages peut laisser à désirer, surtout si les pages originales ont été dactylographiées à l'aide d'un ruban usé ou si l'université nous a fait parvenir une photocopie de qualité inférieure.

La reproduction, même partielle, de cette microforme est soumise à la Loi canadienne sur le droit d'auteur, SRC 1970, c. C-30, et ses amendements subséquents.

Canada

# Force Balancing in a Parallel Redundantly-Actuated Mechanism

Hamid Reza Vaezi

BSc., McGill University, 1990

Department of Electrical Engineering

McGill University

Montréal

May, 1994

A thesis submitted to the Faculty of Graduate Studies and Research
in partial fulfillment of the requirements for the degree of
Master of Engineering

© Hamid Reza Vaezi, 1994

National Library
of Canada

Acquisitions and
Bibliographic Services Branch

395 Wellington Street
Ottawa, Ontario
K1A 0N4

Bibliothèque nationale
du Canada

Direction des acquisitions et
des services bibliographiques

395, rue Wellington
Ottawa (Ontario)
K1A 0N4

*Your file Votre référence*

*Our file Notre référence*

THE AUTHOR HAS GRANTED AN IRREVOCABLE NON-EXCLUSIVE LICENCE ALLOWING THE NATIONAL LIBRARY OF CANADA TO REPRODUCE, LOAN, DISTRIBUTE OR SELL COPIES OF HIS/HER THESIS BY ANY MEANS AND IN ANY FORM OR FORMAT, MAKING THIS THESIS AVAILABLE TO INTERESTED PERSONS.

L'AUTEUR A ACCORDE UNE LICENCE IRREVOCABLE ET NON EXCLUSIVE PERMETTANT A LA BIBLIOTHEQUE NATIONALE DU CANADA DE REPRODUIRE, PRETER, DISTRIBUER OU VENDRE DES COPIES DE SA THESE DE QUELQUE MANIERE ET SOUS QUELQUE FORME QUE CE SOIT POUR METTRE DES EXEMPLAIRES DE CETTE THESE A LA DISPOSITION DES PERSONNE INTERESSEES.

THE AUTHOR RETAINS OWNERSHIP OF THE COPYRIGHT IN HIS/HER THESIS. NEITHER THE THESIS NOR SUBSTANTIAL EXTRACTS FROM IT MAY BE PRINTED OR OTHERWISE REPRODUCED WITHOUT HIS/HER PERMISSION.

L'AUTEUR CONSERVE LA PROPRIETE DU DROIT D'AUTEUR QUI PROTEGE SA THESE. NI LA THESE NI DES EXTRAITS SUBSTANTIELS DE CELLE-CI NE DOIVENT ETRE IMPRIMES OU AUTREMENT REPRODUITS SANS SON AUTORISATION.

ISBN 0-315-99987-X

Canada

*This work is dedicated to my family:*

*To my parents who instilled in me the joy of learning, and*

*To my brothers for their continuous support and kindness*

## Abstract

This thesis presents an implementation of a controller for a redundantly- actuated parallel mechanism.

Firstly, an introduction to the structure and kinematic properties of the parallel mechanism is presented. We begin by describing the **ASI** hydraulic actuator, the main constituents of the mechanism, and move on to review the properties of the whole system. The inverse and forward relationships are derived, and the Jacobian matrix of the system is calculated using velocity analysis.

The controller of the shoulder employs the above properties and relationships to balance for any external forces, in particular the gravity, and to estimate its magnitude. This is done in two steps: damping the motion to rest primarily, and subsequently, determining the bias and actual force vectors in static equilibrium. Finally, the results of the experiments are presented.

The formulation of the optimization of the force distribution problem is then studied. Given an overdetermined system, we present two methods for finding the optimal minimum-norm vector of forces, one in Hilbert space and the other in a generalized complete normed space. The latter is indeed an algorithmic procedure for obtaining a minimum $\infty$-norm or a minimum effort solution, which is a solution of a set of equations whose maximum component's magnitude is the smallest possible. In this method, the dual of problem is solved and then the optimal solution is generated by using concepts from functional analysis.

# Résumé

Cette thèse présente la mise en oeuvre d'un système de commande pour un mécanisme parallèle avec motorisation redondante.

On présente d'abord la structure et les propriétés cinématiques du mécanisme. Les actionneur hydrauliques **ASI** sont décrits, puis les parties constituantes sont discutées ainsi que les propriétés du système complet. Les changements de coordonnées sont dérivés dans les deux sens et la matrice jacobienne est calculée à l'aide de la géometrie vectorielle.

Le système de commande de "l'épaule" met ces propriétés à profit pour equilibrer des forces extérieures arbitraires, en particulier la gravité, et pour en estimer l'intensité. Ceci est fait en deux étapes: amortir les mouvements du système jusqu'à l'arrêt puis estimer le décalage des capteur d'effort. Finalement, on présente des résultats expérimentaux.

On s'occupe ensuite d'optimiser la distribution des efforts, puisqu'il s'agit d'un système surcontraint. On présente deux méthodes pour trouver les vecteurs de norme minimum des forces des actionneurs, une dans un espace de Hilbert, l'autre dans un espace normé genéralisé. Il existe en effet une procédure algorithmique pour calculer des solutions qui minimisent la norme $\infty$. Cette solution minimize la plus grande des componantes de la solution. On résoud un probléme dans l'espace dual et la solution est trouvée à l'aide de concepts d'analyse fonctionnelle.

# Acknowledgements

I would like to express my gratitude to my advisor, Professor Vincent Hayward, for his support, guidance and patience. His depth and breadth of knowledge have been an inspiration throughout this period.

As well, I would like to extend my sincere thanks to my very first advisor, Dr Behnam Bavarian, for his unceasing support, kindness and excellence.

Special thanks to Farzam Ranjbaran for his friendship and numerous hours of insightful discussion. I would also appreciate Duncan Baird and Benoit Boulet for their technical assistance. I am indebted to my other friends who made my stay at McRCIM an enriching experience: thanks to Ali Moosavian, Hamid Rad, Kourosh Etamadi, Jonas Augustand Dan Rey. Lots of thanks to A. Hosseinzadeh for helping me in many occasions, and for his assistance in editing this thesis. I also thank Vincent Hayward for translating Résum e.

Finally, and the most important, I am beholden to my brother, not only because of his efforts, support and generosity, but also for his unflagging affection through ups and downs, his patience in the face of my impetuousness, and his commitment to my success. His brilliance and courage have inspired me throughout my life.

# Claims of Originality

The author of this thesis claims the originality of the following:

1. The implementation of the kinematic properties of the shoulder mechanism
2. The design and implementation of the force coordinator of the mechanism employing its kinematic properties
3. The design and implementation an estimator, to estimate the magnitude of a force acting on the shoulder
4. The implementation of the algorithm to solve for the force optimization problem

# Table of Contents

# List of Figures

# List of Tables

# Chapter 1 Introduction

The past four decades has witnessed the birth and growth of robotics as a distinct discipline in engineering. As a result, robots have come to play an increasing role in industry, and their tasks have become more sophisticated as well. As tasks performed by robots have become more complex and delicate, robotics research has focused on sensor-based robotics, leading to robot controllers with a high degree of complexity required to process vast amounts of data.

Various controllers were developed not only because of task complexity, but also in an attempt to overcome problems that stemmed from current manufacturing robot designs inadequate for many other applications. The precise and delicate control of the end-effector torques and forces is made difficult by the high inertia and the low natural frequency of most manipulators as well as by the friction, backlash in the gearing and transmission systems. Many interesting control algorithms which compute joint torque or force commands, often taking the full nonlinear robot's dynamic model into account, were developed (see, for example [26], [20] and [33]), but few of them have yet been tested and compared experimentally. This is because many robotics research laboratories lack suitable robot manipulator systems with good joint torque control and sensing capabilities [1]. In short, despite many advances, current manipulators are still inadequate for a variety of tasks, most notably those having contact with the environment.

These problems can be remedied in two ways, either by compensation techniques or by the design of manipulators better suited to their environment and tasks. Many of the compensation schemes take the form of control algorithms with force feedback to correct for undesirable nonlinear effects, and lack of performance. In other cases specialized passive mechanisms are introduced, such as compliant wrists, to

provide a tolerance for positioning errors, fast response to environment solicitation and to avoid contact instability. Although this has generated a fair amount of success, it is believed that improved mechanical design of the manipulators themselves is needed to overcome some of the problems with conventional robots.

Most commercially available robots such as the PUMA manipultor consist of serial open loop chains that are well suited for the manipulation of small playloads inside large working space volumes. As discussed by Hayward [11], this type of architecture has a poor weight to load ratio due to the pyramidal effect: "proximal joints must be designed to drive and support the sum of the distal links and joints". The accumulation of errors and lack of rigidity is also unavoidable with this architecture.

This has motivated the development of parallel manipulators, where the end-effector is connected to the base through several closed kinematic chains. Many exmaples of parallel manipulators have been studied. (See [4], [18], [22] and [35], to cite just a few). These manipulators have many advantages over their serial counterparts.

Parallel manipulators possess properties complementary to those of their serial counterparts [17]. They can handle heavy loads and their dynamics are dominated by the dynamics of the actuators and the load. From this standpoint, it seems easier to improve their dynamics by using feedback control since they suffer less from dynamic coupling effects such as those produced by the limbs of serial robots, or from friction, backlash, or joint compliance imputed to transmission devices such as gears or harmonic drives. In the case of platform design, the forces applied by the actuators act on the same rigid endplate and hence they must be coordinated to prevent large internal forces from damaging the manipulator. Moreover, the load's inertial parameters must be estimated or identified, since they affect the overall manipulator dynamics directly. These considerations somewhat complicate controller

design. Unfortunately, this class of manipulators suffers from a small working volume.

To alleviate the above problems, a general purpose manipulator composed of both these architectures would be quite desirable [17]. This idea is inspired from the fact that the properties of parallel manipulators complement those of serial designs. One such design, as described by Hayward [11], consists of a revolute elbow joint interposed between two spherical joints for the shoulder and wrist. The spherical joints are actuated in parallel to provide three degrees of freedom in orientation. This thesis is concerned with the design of a controller and the force distribution in the said spherical joints, to be referred to as shoulder (or wrist).

Shoulders are characterized by their ability to provide for the pointing orientation of manipulator. This characteristic simplifies the kinematics and control, and improves the dynamic properties. Traditional shoulder designs are composed of a serial chain of two or three revolute joints with intersecting axes. These shoulders suffer from the above-explained problems inherent in all serial designs. They also contain unavoidable singularities that seriously reduce the usable workspace [30].

Another method used to eliminate the singularities is based on a mixed serial-parallel shoulder with more than one articulation point [28]. This leads to a complicated design involving chain drives and tension rods that must be fabricated to exacting specifications.

Fully parallel shoulders have been suggested by several authors ( [2] and [10]), however these display small wokspaces that generally limit the utility of the mechanisms.

In recent years the search for robots with improved chracteristics has promoted the development of redundant mechanisms. In that context, redundancy refers to

the addition of more actuators than are strictly necessary for a certain task. For example, positioning and orientating a body in space requires six degrees of freedom, thus a manipulator with seven or more actuated joints is called redundant. Cases of redundancy can be separated into two major categories.

The first and is known as *kinematic redundancy*. Here the additional actuators increase the degrees of freedom of the mechnism giving the capability of self motion. This can be put to a number of uses such as:

- Singularity avoidance [25]
- Minimize joint torques [16]
- Obstacle avoidance [27]

For a detailed discussion of properties of redundancy, the reader is referred to [11].

The second category is known as *actuator redundancy*. For this case the extra actuators do not give added mobility, but are used to control the internal forces in the mechanism. A common example occurs when a multi-fingered hand grasps an object. This may result in an overconstrained problem with more actuators than needed by the force analysis. In the case of grasping, the actuator redundancy is utilized to create friction forces between the load and the fingers, thereby, resulting in a stable grasp [19].

It must be stressed that actuator redundancy can be used within a manipulator itself [29]. Although this is not often done in robots, examples of this abound in nature. The human shoulder is a spherical ball and socket joint actuated by six muscle groups to control three degrees of freedom. Strictly speaking, this is a case of actuator redundancy in which the shoulder muscles are used to supply the internal forces needed to keep the humeral head (ball) firmly anchored to the glenoid socket.

It is the goal of this thesis to introduce a controller for a shoulder mechanism with redundancy. This controller is designed to compensate for and estimate the magnitude of slowly varying external forces applied on the system, in particular gravity with no *a priori* knowledge of the relevant parameters. To the author's knowledge, this is one of the first attempts to design and implement such a controller.

The organization of the thesis is as follows: Chapter 2 presents a general introduction on the hydraulic actuator [7] and kinematic modelling of the shoulder [14]. In chapter 3, a control algorithm and its implementation are described. In chapter 4, the force distribution problem is solved for, and formulated in $l_2$ and $l_\infty$ spaces. Finally, chapter 5 presents the concluding remarks.

# Chapter 2 Introduction to the structure and Kinematics of the Shoulder

This chapter introduces the most important features of the shoulder to provide the reader with sufficient background necessary to follow the material of the next chapters. We begin with describing the physical attributes of the existing prototype. Subsequently, the synthesis of the parallel shoulder will be described. Then the kinematic modelling of the shoulder will be carried out. We begin by introducing the actuator subsystem.

## 2.1 ASI Hydraulic Actuator

This section provides a brief description of the shape and internal structure of a ASI hydraulic actuator, which is a summary of a detailed discussion presented in [8]

The device discussed here is a linear piston-type actuator driven by an integrated high-bandwidth jet pipe suspension valve, and fitted with a force sensor. It is very

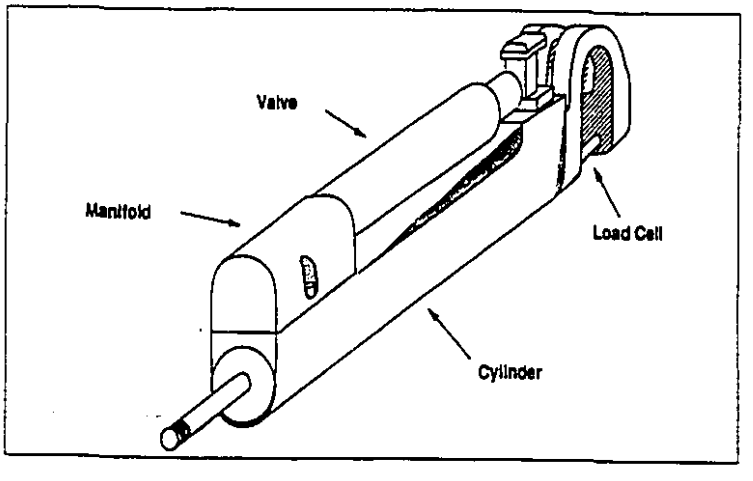


**Figure 2.1:** The hydraulic actuator (adapted from [2])

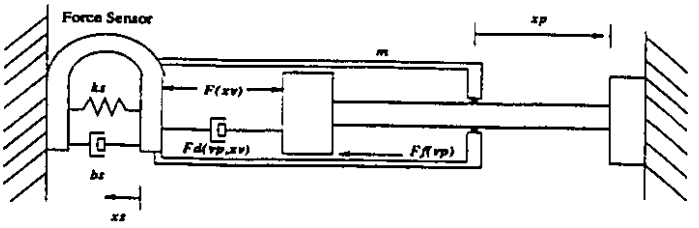


**Figure 2.2:** The actuator model (adapted from [2])

compact, mechanically robust, and its mass is about 0.5 kg. It has an LVDT position sensor as well as a force sensor mounted directly on it. A view of the actuator (without the LVDT position sensor) is shown in Figure 2.1. For a 73 mm stroke, the overall dimensions are 25 × 55 × 139 mm. Since it is a force-controlled device, it must include some elasticity which is almost entirely lumped in the force sensor.

The standard servo system available for the actuator includes a controller card-which can be accessed by a host computer. The card features on-board analog controllers whose valve currents can be specified as desired. The gains can be programmed from a host computer, allowing gain scheduling. The measured state variables can be accessed digitally via an on-board analog to digital converter, allowing for digital control.

These actuators may be essentially seen as force producers. A diagram of the physical actuator model is shown in Figure 2.2. The dynamic and output equations relating the hydraulic force $F$ to the sensed force $F_s$ are:

$$F(x_v) - F_d(x_v, v_p) - F_f(v_p) = m\ddot{x}_s + b_s\dot{x}_s + k_s x_s \tag{2.1}$$

$$F_s = k_s x_s \tag{2.2}$$

where:

$F(x_v)$ = the valve static force

$F_d(x_v, v_p)$ = hydraulic damping force

$F_f(v_p)$ = friction force

$v_p$ = piston velocity

$x_s$ = force sensor deflection

$m$ = actuator mass minus piston mass

$b_s, k_s$ = force sensor paramters

For a more detailed discussion of the above and a model of the servosystem , the reader is refered to [7] and [8].

## 2.2 The Parallel Shoulder

The general case of a fully parallel mechanism consists of a movable platform attached to $n$ legs with one actuator per leg. A point on the platform is then constrained by a spherical joint to prevent translations while permitting freedom of orientation (see Figure 2.3). The spherical joints can be implemented several ways such as gimbals, ball and sockets, or even flexible couplings. The legs are composed of one linear actuator—one cylindrical lower pair—interposed between two Hooke joints, or any other kinematically equivalent arrangement.

Let us denote the center of rotation as $C$, the point of attachment of each leg to the wrist platform as $P_i$, and the point of attachment of each leg to a fixed frame $A_i$, $i = 1, n$. Here we chosen $n = 4$ to make the system redundant.

The use of an additional actuator was proposed in an attempt to reduce or eliminate the singular configurations. Singularities are not the only factor influencing

the size and shape of the workspace. As more actuators are added, there is an increasing chance that they will collide with one another, or with one of the supporting trusses of the mechanism. This tends to decrease the volume of the workspace. For this reason the shoulder was designed with only four actuators which will lead to enough redundancy to eliminate some of the singularities, without causing excessive interference between the legs and trusses.

With actuators, we may think of the mechanism a four sub-mechanism in a combinatorial fashion as in [8]. If one is in a singular configuration the others are not. The attachment points $P_i$ are placed symmetrically in a square with the center being the fixed point $C$.

The geometrical design goal is to enhance cooperation [13]. It can be seen that the workspace limit is reached when either an actuator touches one of the trusses, or when two actuators intersect. By grouping the fixed attachment points in pairs so that $A_1 = A_2$ and $A_3 = A_4$ we eliminate self collisions of the grouped actuators and enlarge the workspace. This leads to the design of Figure 2.4, referred to as the grouped model of a parallel-redundant shoulder. The actual mechanism is shown in Figure 2.5.

The nomenclature for these shoulders, as well as the coordinate frames and variables to be used as part of the kinematic analysis will be defined here. Referring to Figure 2.4:

C: center of rotation of wrist.

$P_i$: Points of attachment of actuators to mobile wrist platform ($i = 1, \ldots, 4$).

$A_i$: Points of attachment of actuators to fixed wrist platform ($i = 1, \ldots, 4$).

$A_p$: Point of attachment of the center post to the fixed wrist platform.

$\mathcal{B}$: Base coordinates centered at C.

$\mathcal{P}$: Coordinates attached to the platform, also centered at C.

$\mathcal{I}$: Intermediate coordinate frame centered at C with axes along the lines $\overrightarrow{A_iC}$

$\vec{n}$: unit vector normal to the mobile wrist platform: $\texttt{unit}\,(\overrightarrow{CP}_2 \times \overrightarrow{CP}_1)$.

${}^{\mathcal{B}}\mathbf{Q}$: Wrist rotation matrix in base coordinates.

$\rho$: wrist actuator lengths, $[\rho_1, \rho_2, \rho_3, \rho_4]^T$, $\rho_i = \|\overrightarrow{A_iP_i}\|$, for $i = 1, \ldots, 4$.

$l_d$: wrist lever length, $l_d = \|\overrightarrow{CP}_i\|$, for $i = 1, \ldots, 4$.

$l_p$: Distance from the plane or the line defined by the $A_i$ to the point C.

$l_b$: Base actuator offset length defined as $\|A_iA_p\|$, for $i = 1, \ldots, 4$.

$\alpha$: The separation angle between $\overrightarrow{A_iA_p}$ and the y-axis of the base frame.

$\omega$: Wrist angular velocity.

$\dot{\rho}$: Wrist actuator velocities, $[\,\dot{\rho}_1 \quad \dot{\rho}_2 \quad \dot{\rho}_3 \quad \dot{\rho}_4\,]^T$.

We adopt the following conventions: The coordinate frames $\mathcal{B}$ and $\mathcal{P}$ are defined with coincidental centers at C, and with z-axes perpendicular to the planes defined by $A_i$ and $P_i$ respectively. The x-axis of the frame $\mathcal{B}$ is parallel to the bisector of angle $\angle A_1A_pA_4$. Similarly, the x-axis of the frame $\mathcal{P}$ is parallel to the bisector of angle $\angle P_1C\ P_4$. With this convention, the frames $\mathcal{B}$ and $\mathcal{P}$ coincide when the manipulator is at the center of the workspace. Upper case letters refer to points and lower case to scalars. Vectors will be written as bold face lower case letters or by letters with overdrawn arrows. Matrices and rotation tensors will be denoted in upper case bold.

## 2.3 Position Analysis of the Parallel Shoulder

The Kinematic modelling of the shoulder was carried out by Hayward and Kurtz [14]. The derivation starts by solving for the so-called forward and inverse kinematics problem. In the forward kinematic problem, the goal is to find the orientation

of the platform in Cartesian coordinates, given the lengths of the actuators. In contrary, the inverse kinematics problem is to find the vector of actuator lengths, given the orientation of the end-effector $X$. This could be specified by the linear invariants of the rotation tensor, quaternions, Euler angles or even by the rotation tensor itself. The rotation tensor was selected because it leads to convenient algebraic manipulation as well as good numerical stability.

For serial robots the forward kinematics problem is simple, but the inverse problem often results in a series of nonlinear equations that are difficult or impossible to solve. The opposite occurs for parallel manipulators: the inverse kinematics is simple, as each kinematic loop contains only a single actuator, but the forward problem can be quite difficult. A closed-form solution exists for the parallel shoulder.

### 2.3.1 Inverse Relationships

The inverse kinematic model is particularly simple to construct by projective geometry. The rotation matrix going from base to end effector coordinates is given by:

$$ {}^{T}\mathbf{S} = \begin{bmatrix} s_{11} & s_{12} & s_{13} \\ s_{21} & s_{22} & s_{23} \\ s_{31} & s_{32} & s_{33} \end{bmatrix} \tag{2.3} $$

We have:

$$ {}^{\mathcal{B}}A_1 = \begin{bmatrix} 0 \\ -l_b \\ -l_p \end{bmatrix} \quad {}^{\mathcal{B}}A_2 = \begin{bmatrix} 0 \\ -l_b \\ -l_p \end{bmatrix} \quad {}^{\mathcal{B}}A_3 = \begin{bmatrix} 0 \\ l_b \\ -l_p \end{bmatrix} \quad {}^{\mathcal{B}}A_4 = \begin{bmatrix} 0 \\ l_b \\ -l_p \end{bmatrix} \tag{2.4} $$

and

$$ {}^{\mathcal{P}}P_1 = \begin{bmatrix} l_d \\ 0 \\ 0 \end{bmatrix} \quad {}^{\mathcal{P}}P_2 = \begin{bmatrix} 0 \\ -l_d \\ 0 \end{bmatrix} \quad {}^{\mathcal{P}}P_3 = \begin{bmatrix} -l_d \\ 0 \\ 0 \end{bmatrix} \quad {}^{\mathcal{P}}P_4 = \begin{bmatrix} 0 \\ l_d \\ 0 \end{bmatrix} \tag{2.5} $$

By coordinate transformation into frame $\mathcal{B}$, we have:

$$ {}^{\mathcal{B}}P_1 = {}^{\mathcal{I}}\mathbf{S}\ {}^{\mathcal{P}}P_1 \quad {}^{\mathcal{B}}P_2 = {}^{\mathcal{I}}\mathbf{S}\ {}^{\mathcal{P}}P_2, \quad {}^{\mathcal{B}}P_3 = {}^{\mathcal{I}}\mathbf{S}\ {}^{\mathcal{P}}P_3, \quad {}^{\mathcal{B}}P_4 = {}^{\mathcal{I}}\mathbf{S}\ {}^{\mathcal{P}}\ P_4 \tag{2.6} $$

thus

$$ \rho_1 = \|{}^{\mathcal{B}}\overrightarrow{P_1A_1}\| = \sqrt{(l_d s_{11})^2 + (l_d s_{21} + l_b)^2 + (l_d s_{31} + l_p)^2} \tag{2.7} $$

$$ \rho_2 = \|{}^{\mathcal{B}}\overrightarrow{P_2A_2}\| = \sqrt{(l_d s_{12})^2 + (l_d s_{22} - l_b)^2 + (-l_d s_{32} + l_p)^2} \tag{2.8} $$

$$ \rho_3 = \|{}^{\mathcal{B}}\overrightarrow{P_3A_3}\| = \sqrt{(l_d s_{11})^2 + (l_d s_{21} + l_b)^2 + (-l_d s_{31} + l_p)^2} \tag{2.9} $$

$$ \rho_4 = \|{}^{\mathcal{B}}\overrightarrow{P_4A_4}\| = \sqrt{(l_d s_{12})^2 + (l_d s_{22} - l_b)^2 + (l_d s_{32} + l_p)^2} \tag{2.10} $$

### 2.3.2 Forward Relationships

The forward kinematics can be found by solving equations (2.7), (2.8), (2.9), and (2.10) for the matrix **S**. Since **S** is orthogonal, its nine elements are subject to six constraints, each row being of unit norm and mutually orthogonal to the other rows. From this we can infer that a rotation can be described by only three variables. Solving for these three variables from the four actuator lengths constitutes a non linear overdetermined system of equations.

Only three of these equations are needed to solve the forward kinematics. If there are errors in our measurement of $\rho$ then we can obtain four different solutions for the rotation variables. Averaging these solutions will help reduce the effects of measurement error on the system. Alternatively, if we assume no measurement errors in $\rho$ then we can use all four values to describe a simple kinematic solution.

From equations (2.7), (2.8), (2.9), and (2.10), we obtain:

$$ l_b\, s_{21} + l_p\, s_{31} = \beta_1, \tag{2.11} $$

$$l_b\, s_{21} - l_p\, s_{31} = \beta_3, \tag{2.12}$$

$$-l_b\, s_{22} - l_p\, s_{32} = \beta_2, \tag{2.13}$$

$$-l_b\, s_{22} + l_p\, s_{32} = \beta_4. \tag{2.14}$$

where $\beta_i = \frac{1}{2l_d}(\rho_i^2 - l_b^2 - l_p^2 - l_d^2), i = 1, ..., 4$. Using Cramer's rule:

$$s_{21} = k_1 \tag{2.15}$$

$$s_{31} = k_2 \tag{2.16}$$

$$s_{22} = k_3 \tag{2.17}$$

$$s_{32} = k_4 \tag{2.18}$$

where $k_1, k_2, k_3, k_4$ are known values. They are:

$$k_1 = (\beta_1 + \beta_3)/2l_b, \quad k_2 = (\beta_1 - \beta_3)/2l_p, \tag{2.19}$$

$$k_3 = (-\beta_2 - \beta_4)/2l_b, \quad k_4 = (-\beta_2 + \beta_4)/2l_p. \tag{2.20}$$

Now we substitute equations (2.15) and (2.16) into the identity $s_{11}^2 + s_{21}^2 + s_{31}^2 \equiv 1$:

$$s_{11}^2 + (k_1^2 + k_2^2 - 1) = 0. \tag{2.21}$$

Solving yields two branches:

$$s_{11} = \pm\sqrt{1 - k_1^2 - k_2^2}. \tag{2.22}$$

From this we can substitute $s_{11}$ back into equation (2.15) to get $s_{21}$. Similarly, using equations (2.17), (2.18) and the identity $s_{12}^2 + s_{22}^2 + s_{32}^2 \equiv 1$, we have:

$$s_{12}^2 + (k_3^2 + k_4^2 - 1) = 0 \tag{2.23}$$

and

$$s_{12} = \pm\sqrt{1 - k_3^2 - k_4^2} \tag{2.24}$$

We then substitute $s_{12}$ back into equation (2.17) to get $s_{22}$. We now have the first and second columns of the rotation matrix **S**, the third column is simply the cross product of the first two.

In general, three of the four branches to this problem will be spurious. Each can be tested by examining the orthogonality constraint $s_{11}s_{12} + s_{21}s_{22} + s_{31}s_{32} \equiv 0$. In certain configurations there will be more than one valid branch. For example, if $k_2 = k_3 = 0$ and $k_4 = 1$ there will be two solutions.

## 2.4 Velocity Analysis

The Jacobian matrix **J** of the inverse kinematic map relates Cartesian velocities to joint rates. The defining equation is:

$$\dot{\rho} = \mathbf{J}\omega. \tag{2.25}$$

The Jacobian of the inverse map will be much easier to solve for than that of the forward one. The actuator velocities can be obtained as linear combinations of the angular velocity by vector geometry. The velocity of point $P_i$ attached to the actuators is:

$$\vec{v}_{P_i} = {}^{\mathcal{B}}\omega \times \overrightarrow{CP_i}. \tag{2.26}$$

The rate of each actuator is the projection of the velocities of the points $P_i$ onto the corresponding line $A_iP_i$. Thus:

$$\vec{a}_i = \overrightarrow{A_iP_i}/\|A_iP_i\| \tag{2.27}$$

$$\dot{\rho}_i = \vec{a}_i \cdot \vec{v}_{P_i} = \vec{a}_i \cdot ({}^{\mathcal{B}}\omega \times \overrightarrow{CP}_i) = {}^{\mathcal{B}}\omega \cdot (\overrightarrow{CP}_i \times \vec{a}_i) \tag{2.28}$$

$$\dot{\rho} = \begin{bmatrix} (\overrightarrow{CP}_1 \times \vec{a}_1)^T \\ (\overrightarrow{CP}_2 \times \vec{a}_2)^T \\ (\overrightarrow{CP}_3 \times \vec{a}_3)^T \\ (\overrightarrow{CP}_4 \times \vec{a}_4)^T \end{bmatrix} {}^{\mathcal{B}}\omega = \mathbf{J}\, {}^{\mathcal{B}}\omega. \tag{2.29}$$

The $4 \times 3$ matrix $\mathbf{J}$ is now explicitly known. After some algebra, the entries of $\mathbf{J}$ are calculated to be as follows:

$$\mathbf{J} = l_d^2 \times \begin{bmatrix} \frac{-s_{21} l_2 - L_1(s_{31}+1)}{\rho_1} & \frac{s_{11} L_2}{\rho_1} & \frac{s_{11} L_1}{\rho_1} \\ \frac{s_{22} L_2 + L_1(s_{32}-1)}{\rho_2} & \frac{-s_{12} L_2}{\rho_2} & \frac{-s_{12} L_1}{\rho_2} \\ \frac{s_{21} L_2 - L_1(s_{31}-1)}{\rho_3} & \frac{-s_{11} L_2}{\rho_3} & \frac{s_{11} L_1}{\rho_3} \\ \frac{-s_{22} L_2 + L_1(s_{32}+1)}{\rho_4} & \frac{s_{12} L_2}{\rho_4} & \frac{-s_{12} L_1}{\rho_4} \end{bmatrix} \tag{2.30}$$

where $L_1 = \frac{l_h}{l_d}$ and $L_2 = 1 - \frac{l_p}{l_d}$.

In addition, the values of the strokes of the actuators must satisfy the following relation ([6], [5]):

$$\begin{aligned} &[(\rho_1^4 + \rho_2^4) - 2\, l_e^2\, (\rho_1^2 + \rho_2^2) + 2\, l_e^4 - 4\, l_o^2\, l_d^2]\, [(\rho_3^4 + \rho_4^4) - 2\, l_e^2\, (\rho_3^2 + \rho_4^2) + 2\, l_e^4 - 4\, l_o^2\, l_d^2] \\ &\quad - [l_e^2\, (\rho_1^2 + \rho_2^2 + \rho_3^2 + \rho_4^2) - (\rho_1^2\, \rho_3^2 + \rho_2^2\, \rho_4^2) - 4\, l_0^2 l_d^2 \cos\mu - 2\, l_e^4]^2 = 0 \end{aligned} \tag{2.31}$$

with $l_0 \equiv \sqrt{l_p^2 + l_b^2}$, $l_e \equiv \sqrt{l_0^2 + l_d^2}$ and $\cos\mu = \sqrt{l_p^2 - l_b^2}/l_0$.

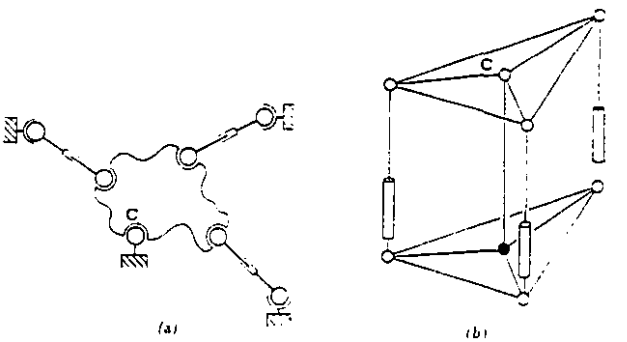


**Figure 2.3:** (a) General case of a fully parallel wrist. The point $C$ is fixed, preventing translations but permitting arbitrary rotations; (b) Symmetric arrangement of a non-redundant wrist consisting of two equilateral triangles, the top one mobile and the bottom one fixed (adapted from [14]).

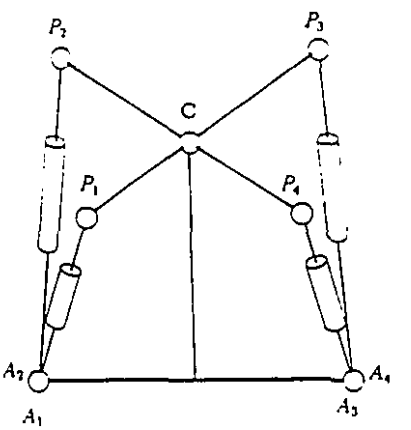


**Figure 2.4:** Schematic arrangement of a grouped actuator redundant manipulator (adapted from [14]).

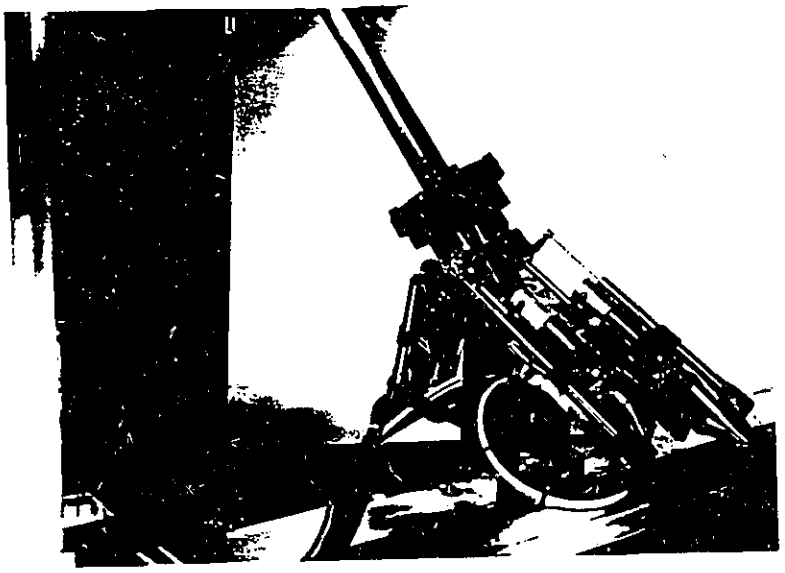

**Figure 2.5:** The parallel redundantly-actuated mechnism (shoulder)

# Chapter 3 Force Balancing in the Parallel Shoulder

The aim of this chapter is to describe the controller of the shoulder. The aim of the controller is to balance any external force exerted on the system, and to estimate its magnitude. The measurements are corrupted with noise, and a time varying bias in the force readings increases the uncertainty of the measurement. Unmodelled linearities are also other factors which perturb these parameters. Despite all the perturbations, the controller must remain stable at all times, and adapt itself to sudden changes in the environment as well. These two properties are emphasized in the shoulder because the inertial parameters may vary dramatically when the manipulator makes contact with the environment or is loaded.

The control system is based on a static model. There is no attempt to model the noise or nonlinearities of the system or to identify their effects. Moreover, the system is not linearized in the vicinity of an operating point. Instead, the motion of the system is damped to rest, and once in a static equilibrium, the magnitude of the force is estimated based on measurements of the torque.

This chapter contains two sections. In the first section, force balancing in a one DOF system is described. Subsequently, it is shown how this simple one DOF system is utilized to design the shoulder's controller.

## 3.1 Control of a 1-DOF Mechanism Using a Hydraulic Actuator

In this section the design of a simple control system for a one DOF system is described. This system is a crank with one hydraulic actuator, and its controller attempts to compensate and estimate the magnitude of any external force imposed

upon it. Since the ultimate goal is to design such a control system for a three DOF system, using four of the same kind of actuators, we found it appropriate to study the behaviour of this one DOF system. To do so, a simple controller was designed in order to gain insight into the properties of the controller. Subsequently, as it will be escribed in the next section, we generalize our findings and apply them to designing a control system of a spherical joint (shoulder).

Presence of an inertia and damping indicate the exertion of an external force. We propose in the following that friction forces are negligible. In particular, compensators with high gain make the friction in the actuator very small even at low velocity. Any unballanced external force can result in an acceleration and velocity in the system. Since calculating acceleration from position measurements is susceptible to noise, acceleration was not considered as a measurable state of the system.

The controller is to balance any external forces, in particular the gravity. This is achieved when a state of static equilibrium is reached. Velocity and force are two state variables to be controlled, however, velocity is the only state variable needed to be measured to achieve static equilibrium. Consider an actuator in this state. Shortly after a perturbation is applied to it, the measured force is not a reliable state variable of this system. As the actutor is made to build up resistance against the perturbing force, the measured force, which is a function of many variables, in a state close to static equilibrium, can be considered as a measurement reflecting the external forces. When the actuator is moving "fast", the force measurement no longer can be used, only velocity can be used.

The structure of this controller is shown as a block diagram in Figure 3.1. In this figure,

$f_d(n)$: the input force

$f_m(n)$: the measured (sensed) force by the actuator

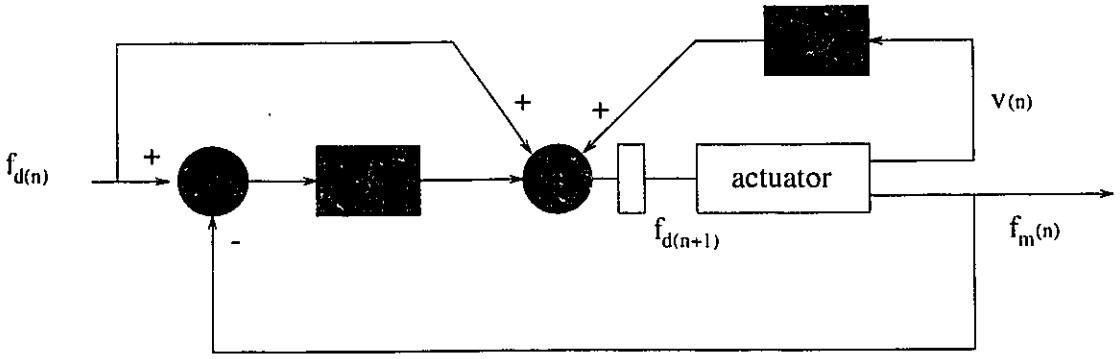


**Figure 3.1:** The coordinator of the crank

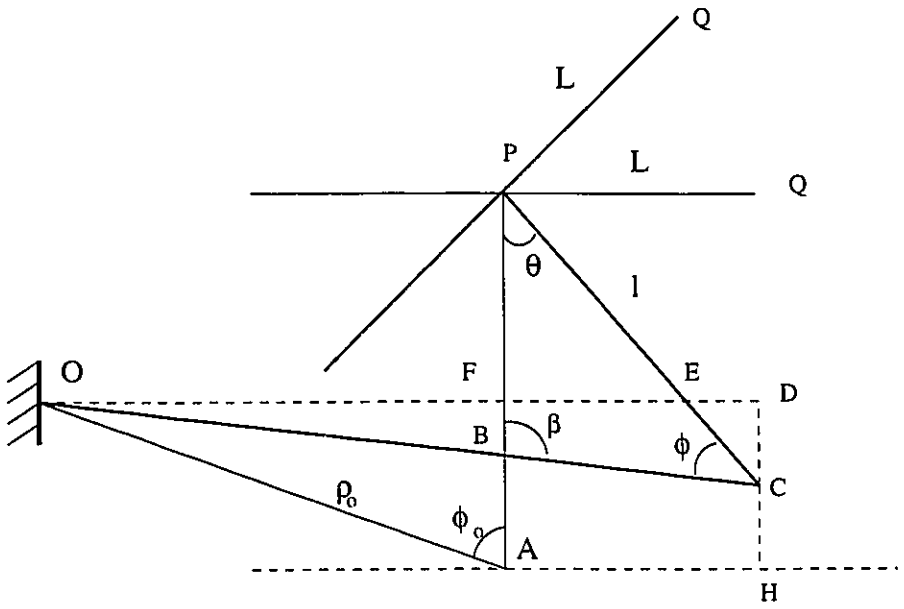


**Figure 3.2:** Abstraction of the geometry of the system

$v(n)$: the linear velocity of the actuator

$K$ and $D$: constant gains

This figure shows a discrete controller with two feedback loops. The external loop feeds back the measured force, $f_m(n)$, into the system, magnifies the difference between the input and output signals, and determines the next input command. In addition, the correction factor $D\,v(n)$ causes damping and forces the system to converge to static equilibrium.

Refering back to Figure 3.1, the closed loop equation of the system is as follows:

$$f_d(n) + K[f_d(n) - f_m(n)] + Dv(n) = f_d(n+1) \tag{3.1}$$

Let the error term be

$$e(n) = f_d(n) - f_m(n) \tag{3.2}$$

then the difference equation describing the error is

$$e(n+1) - (1+K)e(n) = f_m(n+1) - f_m(n) + Dv(n) \tag{3.3}$$

As the state of static equilibrium is reached, the terms $v(n)$ and $f_m(n+1) - f_m(n)$ approach zero, rendering $e(n)$ close to 0. Once $e(n) \approx 0$, $f_m$ represents the actual force exerted on the actuator. However, it must be noted that the force measurement is contaminated by a measurement bias. In section 3 a method to calculate the bias will be described.

Having found $f_m$, the mass of the load, $m$, is calculated from

$$f_m = mg(\frac{L}{l})\cos\theta \sin\phi \tag{3.4}$$

The two constant lengths, $L$.495m and $l = 0.0610$m, and the two variables, $\theta$ and $\phi$ are shown in Figure 3.2. In this figure, $\theta$ is the angle of rotation and $OC$ represents the the actuator with a length of $\rho$. The load is pla[illegible] $Q$ and the arm $PQ$ rotates around $P$. We introduce two new constants $\phi_0 =$ [illegible] degrees and $\rho_0 = .287$m, which are the measured values of $\phi$ and $\rho$, respectively, when $\theta = 0$.

Using the geometric properties of the figure, $\theta$ and $\phi$ can be calculated:

$$\theta = 2\arctan(\frac{1}{2}\frac{2\rho_0 \sin(\phi_0) \pm M}{K + \rho_0 \cos\phi_0 - l})$$

$$\phi = 180 - \arcsin(\frac{l\sin\theta - \rho_0 \sin\phi_0}{\rho}) \tag{3.5}$$

where

$$M = \sqrt{4\rho_0{}^2\sin(\phi_0)^2 - 4K^2 + 4\rho_0{}^2\cos(\phi_0)^2 - 8\rho_0\cos\phi_0 l + 4l^2}$$

The results of three experiments are described. In all the experiments, the actuator is initially at the state of static equilibrium. A weight is placed on the crank, and is left to move freely for 500 milliseconds ($f_d = 0$) so it can pick up velocity. In the first experiment the mass is 2.265 $kg$, whose $f_m = -168$ machine units ($MU$). The mass in the second experiment is 4.530 $kg$, with $f_m = -320$ $MU$. Finally, the third load has a mass of 6.795 $kg$, with $f_m = -479$ $MU$. Notice that because of the kinematics of the system, the force exerted on the endeffector is magnified by a factor of 6 to 8.

There are 3 plots for each experiment. The first one shows the values of $f_m$ and $f_d$. Notice that $f_d = 0$ for the first 0.500 seconds, and then $f_d$ is set to $f_m$. The second plot shows the error $e(n) = f_d(n) - f_m(n)$. Finally, the velocity is plot.

In the first experiment, the crank starts its motion vith no initial velocity. The velocity reaches 5.0 $mm/s$ after 150 milliseconds ($ms$), 8.5 $mm/s$ after 250 $ms$, and remains stable. This velocity is brought to zero in less than 130 $ms$. It is also observed that as the velocity is reduced, $f_d$ and $f_m$ converge toward each other.

A similar pattern is observed in all the experiments. It is seen that the velocity decay rate does not change significantly with different loads. This time decay period can be divided into two parts. The first 200 $ms$ is a period of "coarse tuning", during which the velocity is damped to zero. In the second period "fine tuning" is carried out, and $f_d - f_m$ dominates the input command since the velocity is close to zero.

The above experiments display the main characteristics of the one-actuator controller. These can summarised as following:

- The damper brings the motion of the actuator to zero in a fixed period of time, regardless of the magnitude of the force exerted on it
- There are two processes in damping the motion, which we call, coarse tuning and fine tuning
- "Coarse tuning" brings the velocity close to zero, *i.e.*, compensates for the external forces, but $f_m$ is significantly different from $f_d$.
- "Fine tuning" is the process during which $f_d$ and $f_m$ converge toward each other. After convergence, estimation can be carried out.

The above characteristics will be retained in the design of the controller of the 3 DOF system. As we will see in the next section, this damper is used as one of the main components of the shoulder's control system.

## 3.2 Case of a parallel Mechanism with Actuator Redundancy

In this section, we describe an analogous controller for the spherical joint. As before, the objective is to balance any external force, and estimate its magnitude. As in the case of one DOF system, it is done in two steps. First the static equilibrium is restored to avoid the complexities of analyzing dynamics of the system. Subsequently, the bias vector is calculated and the bias-free force vector is estimated. Thus, the controller is made up of two parts: a damper and an estimator.

The damper is identical to the one introduced in the previous section, with the difference that a coordinator is added to it, to ensure proper distribution of actuator forces. The interaction between the damper and coordinator is shown in Figure 3.6. The coordinator serves to monitor and modify the output of the damper.

The particular functions of the controller are:

- Force balancing: compensates for the external force imposed on the system by damping the velocity
- Force optimization: optimizes the forces of the actuators at the state of static equilibrium
- Load estimation: estimates the magnitude of the external force

The controller also avoids certain configurations in which the structure or the actuators may be physically damaged. For this reason, the safety of the system is checked at every stage and at each iteration.

The block diagram of the controller is shown in Figure 3.7. The final output is $F_d(n)$ which is produced by only one of the three possibilities shown in the figure. Refering to this figure, the above functions will be explained in more details, in the coming subsections.

## 3.3 Force Compensation

The task of the coordinator is to scale the input force command of each actuator, which has been calculated by the damper. It compares the outputs of actuators with each other, and calculates a weight for each input command. In addition, the coordinator is to identify the actuator(s) which are not operating in harmony with the rest and reduces the input force to that (those) actuator(s). This scaling operation of the controller is based on monitoring the velocity history of an actuator, and comparing the velocities of all the actuators. As a result, a smooth damping is carried out.

### 3.3.1 Force Optimization

Because the mechanism is actuator redundant, there exists an infinite number of actuator force combinations which all produce a given force output. A systematic method to select one particular solution consists of minimizing the norm of the force vector. Depending upon the mathematical technique employed, this will be carried out either in $l_2$ or $l_\infty$. The optimization techniques will be dealt with in more detail in the next chapter.

### 3.3.2 Force Estimation

Force or load estimation is the last stage. The output of this stage is the value of the magnitude of the external force applied at the endeffector. This value is calculated from the torque and the Jacobian of the system.

The external force is assumed to be a load, quasi-statically supported by the shoulder mechanism. Therefore, the direction of the force is always taken parallel to a vertical axis. It is also assumed that the force is exerted on the endeffector only. The reason is that one can easily define a position vector from the joint to the endeffector whose norm is constant.

Accurate estimation of the load requires prior calculation of the force sensor bias. The bias may be seen as a persistent disturbance on the system. In general, however, it will vary slowly with time. The bias is represented as a constant vector since the estimation occurs within a few seconds, a short time as compared to the time of sensor drift.

We refer back to

$$\tau_m = \mathbf{J}^T \mathbf{f}_m \tag{3.6}$$

where $\tau_m$ is the torque balancing the actuator measured forces $\mathbf{f}_m$. The vector $\mathbf{f}_m$ can

be decomposed into two vectors:

$$\mathbf{f}_m = \mathbf{f} + \mathbf{b} \tag{3.7}$$

$\mathbf{f}$ and $\mathbf{b}$ are $4 \times 1$ real vectors and represent the actual force and the bias, respectively. The goal is to estimate $\mathbf{b}$, given $\mathbf{f}_m$.

Referring to the previos chapter, we define two frames of reference. The first one is has an origin which coincides with the center of the rectangle $A_1A_2A_3A_4$. This is the inertial frame denoted by $O_0X_0Y_0Z_0$. Another frame of reference, denoted by $O_1X_1Y_1Z_1$ with $Z_1$ overlaping $Z_0$. $X_1$ and $Y_1$ are obtained by rotating $X_0$ and $Y_0$ around the $Z_0$axis respectively, by 45 degrees. The rotation matrix going from base to the endeffector coordinates is given by

$$^{\mathcal{I}}\mathbf{Q} = {}^{\mathcal{I}}\mathbf{S}R \tag{3.8}$$

$^{\mathcal{I}}\mathbf{S}$ is calculated as shown in the previous chapter and

$$R = \begin{bmatrix} \frac{1}{\sqrt{2}} & -\frac{1}{\sqrt{2}} & 0 \\ \frac{1}{\sqrt{2}} & \frac{1}{\sqrt{2}} & 0 \\ 0 & 0 & 1 \end{bmatrix} \tag{3.9}$$

A vector v fixed in the moving frame, for example, is expressed in the inertial frame as:

$$^{\mathcal{I}}p = {}^{\mathcal{I}}\mathbf{Q}\,{}^{\mathcal{P}}p \tag{3.10}$$

Let $^{\mathcal{P}}p$ be the position vector connecting $O_1$ and the endeffector, $E$. It is a vector with coordinates

$$^{\mathcal{P}}p = \begin{bmatrix} l \\ l \\ h \end{bmatrix} \tag{3.11}$$

A mass $m$, placed at $E$, exerts the force f

$$\mathrm{f} = m\mathrm{g} = m \begin{bmatrix} 0 \\ 0 \\ -g \end{bmatrix} \tag{3.12}$$

where g is the acceleration vector due to gravity, and $g = 9.81 m/s^2$.

In *static equilibrium*, a force f results in a torque $\tau$ around a line passing through $O_1$:

$$\tau = \mathrm{f} \times {}^{\mathcal{I}}P = \mathrm{f}^T \begin{bmatrix} 0 & -P_{z_0} & P_{y_0} \\ P_{z_0} & 0 & -P_{x_0} \\ -P_{y_0} & P_{x_0} & 0 \end{bmatrix} \tag{3.13}$$

Since the above matrix is skew-symmetric, it is singular. Furthermore, it can be shown that its rank is 2. Therefore, one of its rows is linear combination of the other two rows, and because its skew-symmetry property, one of its columns can also be written as a linear conbination of the other two. Let's denote the three columns of this matix as $\mathbf{P}_1$, $\mathbf{P}_2$ and $\mathbf{P}_3$. Then

$$\mathbf{P}_3 = k_1\mathbf{P}_1 + k_2\mathbf{P}_2$$

for $k_1 = -\frac{P_{x_0}}{P_{z_0}}$ and $k_2 = -\frac{P_{y_0}}{P_{z_0}}$. Equation (3.13) is rewritten as

$$\tau = \begin{bmatrix} \mathrm{f}^T\mathbf{P}_1 \\ \mathrm{f}^T\mathbf{P}_2 \\ \mathrm{f}^T(k_1\mathbf{P}_1 + k_2\mathbf{P}_2) \end{bmatrix} \tag{3.14}$$

where f is the actual force of the load and $\tau$ is its resulting torque. Therefore, for any f, there is a $\tau$ (expressed in the inertial frame) whose components have the fol-

lowing relationship:

$$\tau_{z_0} = k_1 \tau_{x_0} + k_2 \tau_{y_0} \tag{3.15}$$

On the other hand, considering the particular f form (3.12),

$$\tau = \mathbf{f} \times {}^{T}P = \begin{bmatrix} m P_{y_0} \\ -m P_{x_0} \\ 0 \end{bmatrix} \tag{3.16}$$

From (3.16), (3.15) is readily verified. Moreover, since $\tau_{z_0} = 0$:

$$\tau_{y_0} = k \tau_{x_0} \tag{3.17}$$

In the presence of the measuremant bias, using (3.7):

$$\tau_m = \tau + \tau_b = \mathbf{J}^T \mathbf{f} + \mathbf{J}^T \mathbf{b} \tag{3.18}$$

$\tau$ represents the static torque ( as obtained above), and $\tau_b$ the torque due to the bias. Since **b** is a $4 \times 1$ vector, and is assumed to be constant, we need four equations to exactly identify it. Expressing **J** by its columns as $[\mathbf{J}_1\, \mathbf{J}_2\, \mathbf{J}_3]$, from(3.17), the following two relations can be derived for the static torque,$\tau$, with every measurement of $\tau_m$:

$$(\mathbf{J}_2 - k\mathbf{J}_1)\mathbf{b} = \tau_{m_{y_0}} - k\tau_{m_{x_0}} \tag{3.19}$$

and from (3.16),

$$\tau_{m_{z_0}} = \mathbf{J}_3 \mathbf{b} \tag{3.20}$$

Measuring $\tau_m$ in two different positions at equilibrium provides the four equations needed to calculate b. The goal, at this stage, is to find $m$. Once **b** is determined, equation (3.16) may be used to calculate $m$.

Table 3.1 shows the mass of several loads and their estimated values calculated using the above method. It is noticed that as the mass increases, the estimation be-

| Actual Mass (Kg) | Average estimated mass (Kg) | % error |
|---|---|---|
| 1.000 | 1.129 | 12.9 |
| 2.265 | 2.541 | 12.2 |
| 4.000 | 4.419 | 10.5 |
| 4.530 | 5.014 | 10.7 |
| 6.265 | 6.907 | 10.0 |
| 8.530 | 9.377 | 9.9 |

**Table 3.1:** The actual masses and their average estimated values

comes more accurate. This is due to an increase in the signal to noise ratio ($SNR$). However, we notice that the decrease in error is not inversely proportional to the increase in the load. This indicates that the magnitude of the noise is significantly low, and the measurements, although contaminated by the noise, are reliably accurate. The error of 10% in all the estimations is a scaling error. This error can be significantly reduced if the system is recaliberated more carefully.

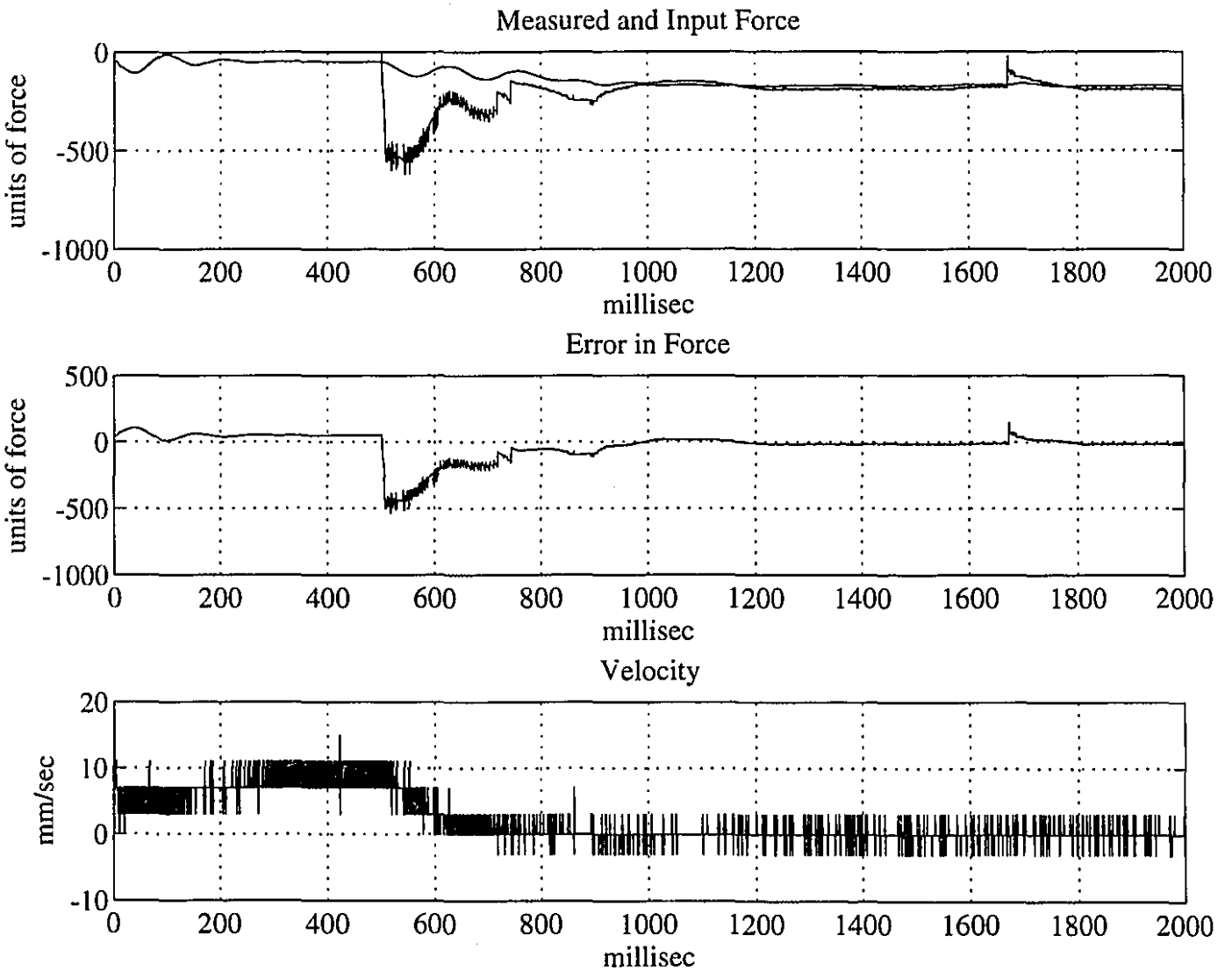


**Figure 3.3:** The plots of responses of the system versus time. The mass of the load is 2.265 $kg$, equal to -168 machine units.

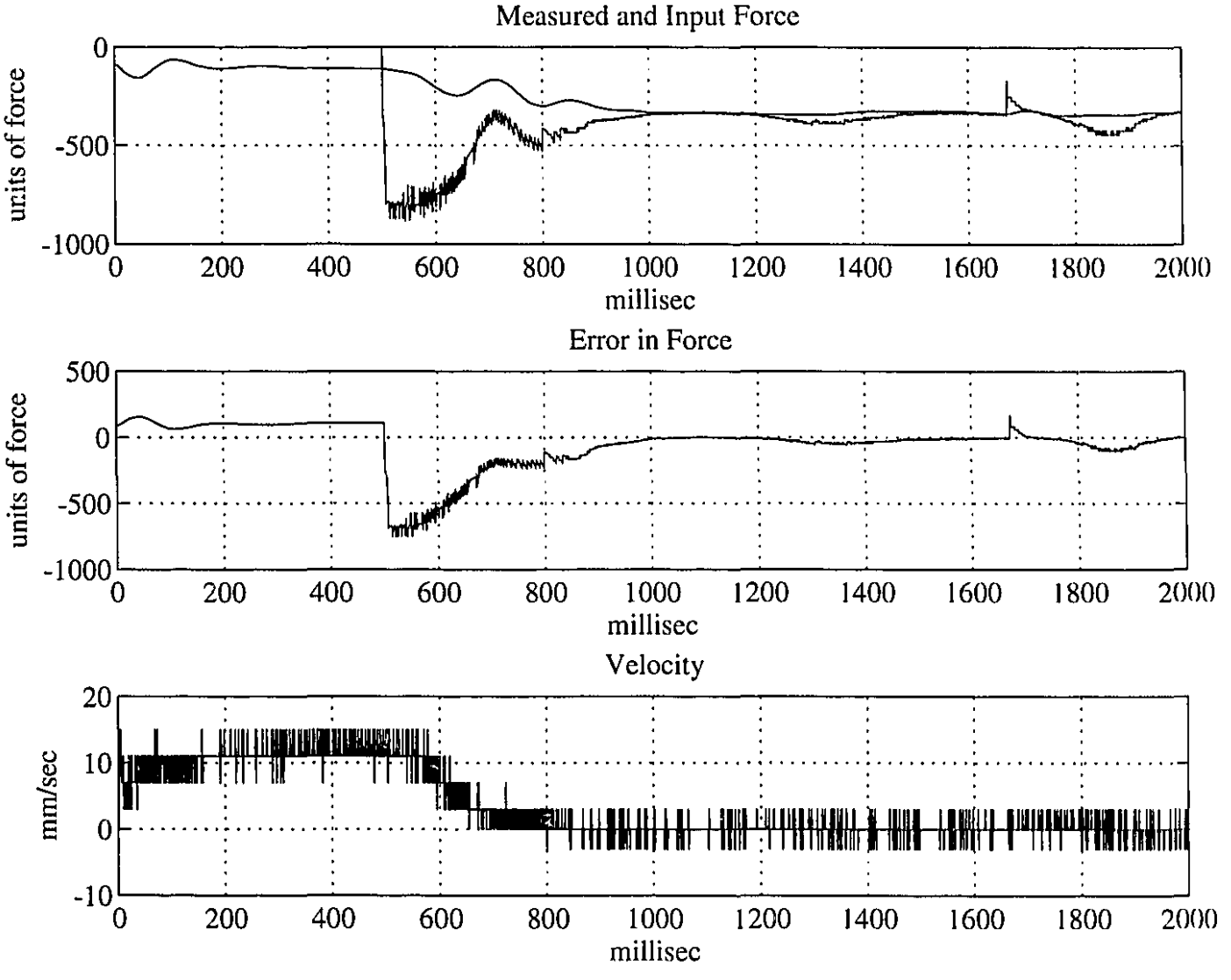


**Figure 3.4:** The plots of responses of the system to a load of mass 4.530 $kg$, equal to -320 machine units.

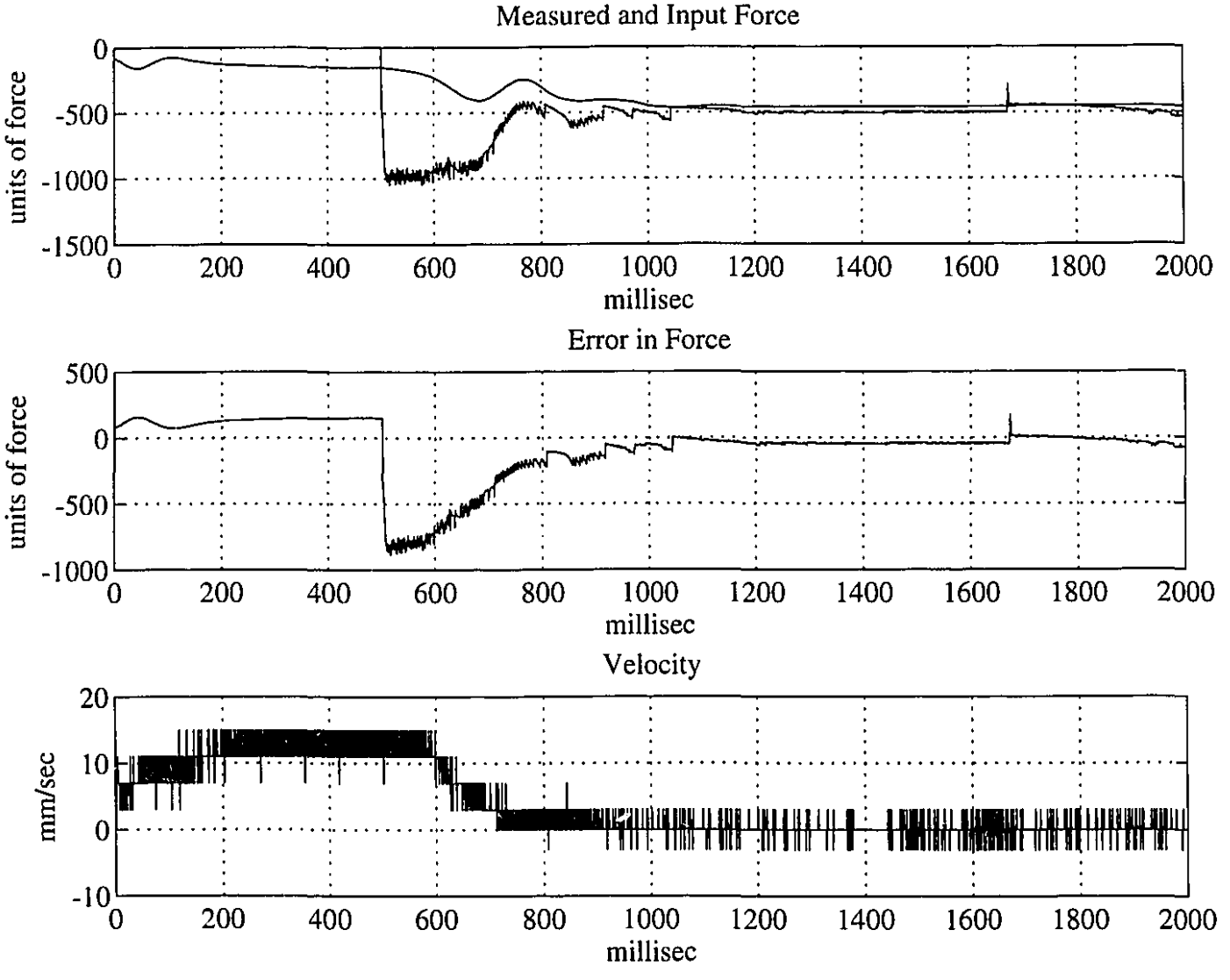


**Figure 3.5:** The plots of responses of the system to a load of mass 6.795 *lbs*, equal to -480 machine units.

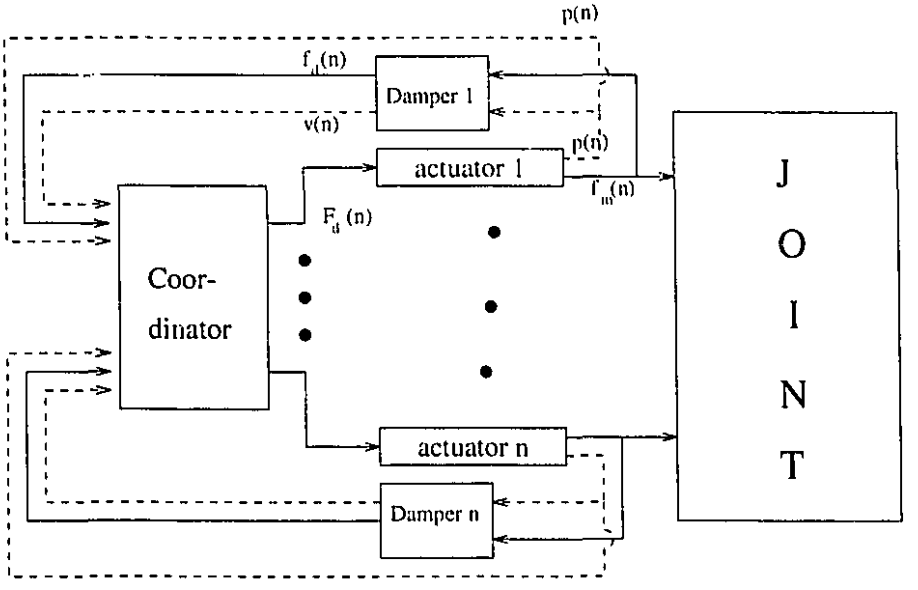


**Figure 3.6:** The damper and coordinator, and their interaction in the shoulder's controller

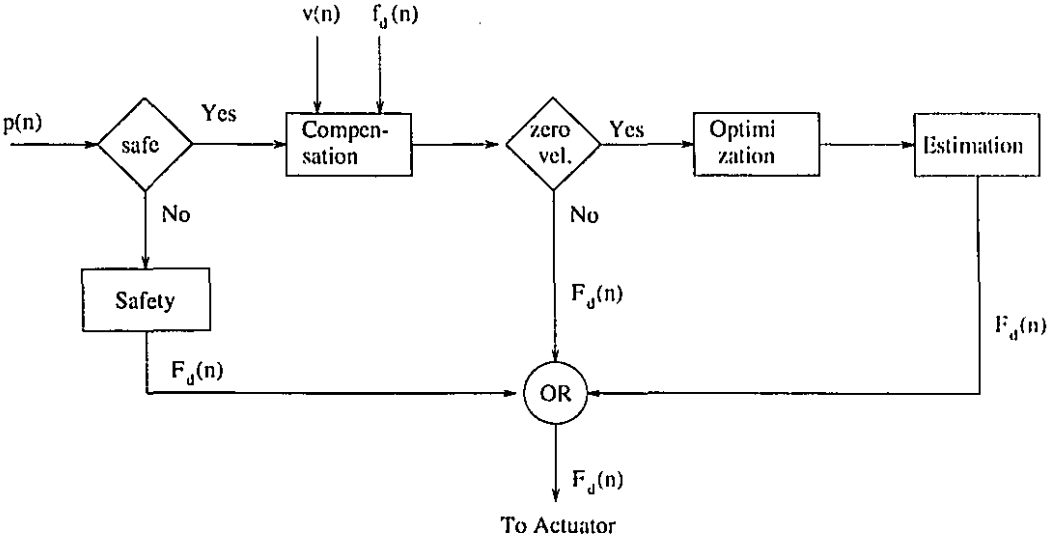


**Figure 3.7:** The controller and its contituents

# Chapter 4 Optimization of the Shoulder's Actuator Forces

## 4.1 Introduction

The joint output torques are related to the actuator forces by the transpose of the Jacobian:

$$\tau = \mathbf{J}^T \mathbf{f} \tag{4.1}$$

where $\tau \in \Re^3$ and $\mathbf{f} = [f_1 \quad f_2 \quad f_3 \quad f_4]^T \in \Re^4$. Given $\tau$ and $\mathbf{J}$, one can find an infinite number of solutions for the above equation. As in [7], here we shall present two methods for finding the minimum norm optimal solution according to two different definitions of the norm, one in Hilbert space and the other in Banach space.

The first optimization problem may be stated as follows: given the relationship between $\tau$ and $\mathbf{f}$, find the optimal minimum-norm vector $\tilde{\mathbf{f}}$ that satisfies it when the norm is chosen to be the usual Hilbert space norm:

$$\|\mathbf{f}\| = (\sum_{i=1}^{4} f_i^2)^{1/2}. \tag{4.2}$$

The minimum 2-norm optimal vector of actuators corresponds to the solution of (4.1), obtained by using pseudo-inverse of the transposed Jacobian $\mathbf{J}^T$. The optimal vector is calculated as

$$\tilde{\mathbf{f}} = \mathbf{J}(\mathbf{J}^T\mathbf{J})^{-1}\tau \tag{4.3}$$

where $\tilde{\mathbf{f}}$ is the minimum vector satisfying (4.1) when the norm is defined as in (4.2). The second minimum norm optimization problem is formulated in a Banach space as it will be explained in the next section.

## 4.2 Minimum $\infty$-norm Optimal Vector of Forces

Many optimization problems in engineering can be put in the form:

$$\min \quad [\max(|f_1|, |f_2|, \cdots, |f_n|)] \stackrel{\text{def}}{=} \min \|\mathbf{f}\|_\infty \tag{4.4}$$

$$\text{subject to:} \quad \mathbf{g} = \mathbf{J}^T \mathbf{f} \tag{4.5}$$

$$0 < n < m, \mathbf{f} \in \Re^n \text{ and } \mathbf{g} \in \Re^m$$

The solution to the above problem solves a "minimum-effort" underconstrained problem in the sense that it will select the solution which achieves the smallest possible inputs taken individually. In other terms, given bounds on the inputs, it will maximize the output.

To solve the problem, we formulate it in a dual space, and use some basic concepts from functional analysis, as described by Luenberger in [24], which will be presented in the next subsection.

### 4.2.1 Basic Concepts and Definitions

The dual space of linear functionals of a normed space is the generalized form of the inner product in Hilbert space. Moreover, the projection theorem, which gives the solution to minimum-norm problems in Hilbert space, can be extended to arbitrary Banach spaces.

First, recall that $l_p$ spaces are spaces of infinite sequences of real numbers with norm defined as

$$\|\boldsymbol{x}\|_p = \left( \sum_{i=1}^{+\infty} |x_i|^p \right)^{1/p}, \tag{4.6}$$

$$\text{where} \quad \boldsymbol{x} \in l_p, \quad \boldsymbol{x} = \{x_1, x_2, x_3, \ldots\}, \quad x_i, p \in \Re, \quad 1 \leq p < +\infty.$$

For $p = +\infty$, the $l_\infty$ space is the space of bounded sequences of real numbers, and the norm is defined as

$$\|\boldsymbol{x}\|_\infty = \sup_i |x_i|. \tag{4.7}$$

Our purpose will be to use a subspace of $l_1$ in which not all the vectors identically zero, and also a subspace of $l_\infty$ defined similarly. Also needed is the following definition of a normed dual space.

**Definition 4.1** *Let $\mathcal{X}$ be a normed linear vector space. The space of all bounded linear functionals on $\mathcal{X}$ is called the* normed dual *of $\mathcal{X}$ and is denoted as $\mathcal{X}^*$. The norm of an element $\boldsymbol{x}^* \in \mathcal{X}^*$ is defined as*

$$\|\boldsymbol{x}^*\| = \sup_{\|\boldsymbol{x}\| \leq 1} |\boldsymbol{x}^*(\boldsymbol{x})|, \tag{4.8}$$

*where $\boldsymbol{x}^*(\boldsymbol{x})$ denotes the value of the linear functional $\boldsymbol{x}^*$ at $\boldsymbol{x} \in \mathcal{X}$ .*

The value of $\boldsymbol{x}^*$ at $\boldsymbol{x} \in \mathcal{X}$ will also be denoted by $\langle \boldsymbol{x}^*, \boldsymbol{x} \rangle$ or by $\langle \boldsymbol{x}, \boldsymbol{x}^* \rangle$ to suggest the analogy with the inner product in Hilbert space.

We are now ready to show that the normed dual space $\mathcal{X}^*$ of the space $\mathcal{X}$ of real numbers $\boldsymbol{x} = (\eta_1, \eta_2, \ldots)$ with norm defined as $\|\boldsymbol{x}\|_1 = \sum_{i=1}^{\infty} |\eta_i|$ is the space of real numbers $\boldsymbol{y} = (\beta_1, \beta_2, \ldots)$ with norm defined in 4.4.

**Proposition 1** *The normed dual space $\mathcal{X}^*$ of the space $\mathcal{X}$ of all of real numbers with norm defined as*

$$\|\boldsymbol{x}\|_1 = \sum_{i=1}^{\infty} |\eta_i|, \tag{4.9}$$

$$\textit{where} \qquad \boldsymbol{x} = (\eta_1, \eta_2, \ldots) \in \mathcal{X},$$

*is the space of real numbers $\boldsymbol{y} = (\beta_1, \beta_2, \ldots)$ with norm defined as*

$$\|\boldsymbol{x}^*\| = \|\boldsymbol{y}\|_\infty = \max_{i=1,2,\ldots} |\beta_i|. \tag{4.10}$$

*Moreover, the value of* $x^*$ *at* $x$ *can be expressed as*

$$\langle x^*, x \rangle = \sum_{i=1}^{\infty} \beta_i \eta_i. \tag{4.11}$$

Proof of the above is presented in Chapter 5 of [24].

The transposed jacobian $J^T$ in (4.5) will be regarded as an element of $\mathcal{X}$ while $f$ will be considered as belonging to $\mathcal{X}^*$. Equation 4.5 can be rewritten as

$$\langle f, J^T \rangle = \mathrm{g}. \tag{4.12}$$

Now the problem is: find an $f \in \mathcal{X}^*$ such that (4.12) is satisfied and $\|f\|_\infty$ is minimum. The existence of this minimum-norm vector is guaranteed by virtue of theorem 2, Section 5.8 of [24]. We continue our discussion by stating the following definitions of alignment and orthogonality properties in dual spaces.

**Definition 4.2** *A vector* $x^* \in \mathcal{X}^*$ *is said to be* aligned *with a vector* $x \in \mathcal{X}$ *if* $\langle x^*, x \rangle = \|x^*\|\|x\|$.

**Definition 4.3** *The vectors* $x^* \in \mathcal{X}^*$ *and* $x \in \mathcal{X}$ *are said to be* orthogonal *if* $\langle x^*, x \rangle = 0$.

The solution to (4.5) can be obtained using the following theorem from [24]:

**Theorem 1**

$$d = \min_{\langle \mathrm{f}, J^T \rangle = \mathrm{g}} \|f\| = \max_{\|\mathrm{a}^T J^T\|_1 \leq 1} \langle \bar{f}, \mathrm{a}^T J^T \rangle = \max_{\|\mathrm{a}^T J^T\|_1 \leq 1} \mathrm{a.g}, \tag{4.13}$$

$$\textit{where } \bar{f} \textit{ satisfies } \langle \bar{f}, J^T \rangle = \mathrm{g}.$$

*Furthermore, the optimal vector* $\tilde{f}$ *is aligned with the optimal* $\mathrm{a}^T J^T$, *i.e.*

$$\langle \tilde{f}, \mathrm{a} J^T \rangle = \|\tilde{f}\|_\infty \|\mathrm{a}^T J^T\|_1. \tag{4.14}$$

$\mathbf{a}$, in the above equation, is a vector whose dimension is equal to that of $\mathbf{g}$, *i.e.*, $\mathbf{a} \in \Re^n$. (4.14) can be rewritten as

$$\max < \tilde{\mathbf{f}}, \mathbf{a}^T\mathbf{J}^T >= \|\tilde{\mathbf{f}}\|_\infty \|\mathbf{a}^T\mathbf{J}^T\|_1 = \max(\mathbf{ag}) \tag{4.15}$$

subject to $< \mathbf{f}, \mathbf{J}^T >= \mathbf{g}$ and $\|\mathbf{a}^T\mathbf{J}^T\|_1 \leq 1$.

### 4.2.2 Minimum $\infty$-norm Optimal Vector of Forces

In this section an algorithm is presented to find $\tilde{\mathbf{f}}$ by solving (4.14). This algorithm is based on the following theorem, which has been proposed and proven by Cadzow [9]. We have adapted the original notation to our notation.

**Theorem 2** *Given the $m \times n$ matrix $\mathbf{J}^T$ with rank $m$ and the $m \times 1$ vector $\mathbf{g}$, there exists an $m \times 1$ vector $\mathbf{a}_0$ such that*

$$\mathbf{g}^T\mathbf{a}_0 = \max(\mathbf{g}^T\mathbf{a}) \quad subject\ to\ \|\mathbf{Ja}\|_1 = 1$$

*at least $m-1$ components of $\mathbf{Ja}_0$ are zero. That is,*

$$\mathbf{J}_i{}^T\mathbf{a}_0 = 0, \quad for\ \ i \in \Omega = \{i_1, i_2, \cdots, i_{m-1}\} \quad with\ \ 1 \leq i_k \leq n \tag{4.16}$$

*$\mathbf{J}_i$ is the $i$th column of the matrix $\mathbf{J}$. Furthermore, the set of vectors $\{\mathbf{J}_{i_1}, \mathbf{J}_{i_2}, \cdots, \mathbf{J}_{i_{m-1}}\}$ are linearly independent.*

Based on the results of (4.15) and Theorem 2, a method for determining a solution to the $\infty$-norm problem is available. Specifically, one sets to zero $m-1$ components of $\mathbf{Ja}$ which correspond to linearly independent rows of $\mathbf{J}$. This generates a set of $m-1$ linear relationships between the coefficients $a_1, a_2, \cdots, a_m$. From these

relationships one determines the optimal values of the $a_i$ so that the $\mathbf{g}^T\mathbf{a}$ is maximized. After performing this iteration on all possible combinations of $m-1$ linearly independent rows of $\mathbf{J}^T$, the optimal value of $\|\tilde{\mathbf{f}}\|_\infty$ is given by the maximum value of the $\mathbf{g}^T\mathbf{a}$ generated this way. Then the alignment property is used to obtain $\mathbf{f}_0$.

Now we will elaborate on the details of the procedure for carrying out the above algorithm. To illustrate the first cycle of the iteration it will be assumed that the first $m-1$ rows of $\mathbf{J}$ are linearly independent.

We now partition the $n \times m$ $\mathbf{J}$ matrix into two blocks as follows:

$$\mathbf{J} = \begin{bmatrix} \mathbf{J}_1 \\ \mathbf{J}_2 \end{bmatrix} \tag{4.17}$$

where $\mathbf{J}_1$ is an $(m-1)\times m$ matrix of rank $m-1$ while $\mathbf{J}_2$ is an $(n-m+1)\times m$ matrix. Setting the first $m-1$ components of $\mathbf{Ja}$ to zero requires that the $m-1$ vector $\mathbf{a}$ be orthogonal to each of $\mathbf{J}_1$ rows. Since the rank of $\mathbf{J}_1$ is $m-1$, the vector $\mathbf{a}$ must lie in a vector subspace of dimension one. Let $\mathbf{h}$ be a basis vector for this space, that is,

$$\mathbf{J}^T\mathbf{h} = 0, \qquad i = 1, 2, \cdots, m-1. \tag{4.18}$$

Since the maximization of $\mathbf{Ja}$ requires that $\|\mathbf{Ja}\|_1 = 1$, one has, for $\mathbf{a} = c\mathbf{h}$, $c \in \Re$,

$$\|\mathbf{Ja}\|_1 = \|\mathbf{Jah}\|_1 = |c|\,\|\mathbf{Jh}\|_1 = 1 \tag{4.19}$$

or

$$|c| = \frac{1}{\|\mathbf{Jh}\|_1} \tag{4.20}$$

The criterion to be maximized becomes

$$\mathbf{g}^T\mathbf{a} = a\mathbf{g}^T\mathbf{h}. \tag{4.21}$$

Expression (4.20) gives the magnitude of the optimal choice of $c$ while (4.21) gives the proper sign of $c$, that is

$$c = \frac{sgn(\mathbf{g}^T\mathbf{h})}{\|\mathbf{J}\mathbf{h}\|_1}.$$

Therefore,

$$\mathbf{a}_0 = \frac{sgn(\mathbf{g}^T\mathbf{h})}{\|\mathbf{J}\mathbf{h}\|_1}\mathbf{h} \tag{4.22}$$

and the criterion to be maximized is

$$\mathbf{g}^T\mathbf{a}_0 = \frac{|\mathbf{g}^T\mathbf{h}|}{\|\mathbf{J}\mathbf{h}\|_1} \tag{4.23}$$

This is the maximum value which $\mathbf{g}^T\mathbf{a}$ may take on if the first $m-1$ components of $\mathbf{J}\mathbf{a}$ are constrained to be zero and $\|\mathbf{J}\mathbf{a}\|_1 = 1$.

This method is next carried out for all other sets of $m-1$ components of $\mathbf{J}\mathbf{a}$ corresponding to linearly independent rows of $\mathbf{J}$. The systematic procedure to be followed is now outlined. The algorithm, adapted from [9], consists of six steps as following:

*Step 1):* Determine all possible combinations of $m-1$ rows from the matrix $\mathbf{J}$ which form a set of linearly independent vectors. Let there be a total of $N$ such combinations. The maximum value that $N$ can take on is $\begin{pmatrix} n \\ m-1 \end{pmatrix}$. Thus there corresponds a set of $N$ different $m \times 1$ $\mathbf{h}$ vectors, that is $\mathbf{h}_1, \mathbf{h}_2, \cdots, \mathbf{h}_N$. These are computed *a priori* and stored in memory. If there are two vectors which are linearly dependent in this set, then one may be discarded as each leads to the same set of components of $\mathbf{J}\mathbf{a}$ being zero. Therefore, one needs only retain the largest subset of that set whose elements are pairwise independent.

*Step 2):* Given the $m \times 1$ vector $y$, one computes

$$\{\mathbf{g}^T\mathbf{a}_0\}_i = \frac{|\mathbf{g}^T\mathbf{h}_i|}{\|\mathbf{J}\mathbf{h}_i\|_1} \qquad i = 1, 2, \cdots, N \tag{4.24}$$

where the scalars $\|\mathbf{J}\mathbf{h}_i\|_1$ are computed *a priori* and stored. It is possible to normalize $\mathrm{h}_i$'s so that $\|\mathbf{J}\mathbf{h}_i\|_1 = 1$.

*Step 3):* Determine the maximum of the $\{\mathrm{g}^T\mathrm{a}_0\}_i$, that is,

$$\|\mathrm{f}_0\|_\infty = \{\mathrm{g}^T\mathrm{a}_0\}_q = \max[\{\mathrm{g}^T\mathrm{a}_0\}_1, \{\mathrm{g}^T\mathrm{a}_0\}_2, \cdots, \{\mathrm{g}^T\mathrm{a}_0\}_N]. \tag{4.25}$$

*Step 4):* An optimal selection of a is then given by

$$\mathrm{a}_0 = \frac{sgn(\mathrm{g}^T\mathrm{h}_q)}{\|\mathbf{J}\mathrm{h}_q\|_1}\mathrm{h}_q \tag{4.26}$$

$$\mathbf{J}\mathrm{a}_0 = \frac{sgn(\mathrm{g}^T\mathrm{h}_q)}{\|\mathbf{J}\mathrm{h}_q\|_1}\mathbf{J}\mathrm{h}_q \tag{4.27}$$

*Step 5):* Use the fact that $\mathrm{f}_0$ and $\mathbf{J}\mathrm{a}_0$ are aligned to compute $\mathrm{f}_0$. Hence, we can write

$$\mathrm{f}_{0_i} = \|\mathrm{f}_0\|_\infty sgn[\mathbf{J}\mathrm{a}_0]_i = \frac{|(\mathrm{g}^T\mathrm{h}_q)|}{\|\mathbf{J}\mathrm{h}_q\|_1} sgn[\mathbf{J}\mathrm{a}_0]_i, \qquad for \;\; [\mathbf{J}\mathrm{h}_q]_i \neq 0 \tag{4.28}$$

while those components of $\mathrm{f}_{i_0}$, for $[\mathbf{J}\mathrm{h}_q]_i = 0$, are obtained in the following manner.

*Step 6):* Substitution of the optimal values of $\mathrm{f}_{i_0}$, for those $i$ for which $[\mathbf{J}\mathrm{h}_q]_i \neq 0$, into the equation $\mathbf{J}^T\mathrm{f} = \mathrm{g}$ leads to a set of $m$ equations in $r$ unknowns $\hat{\mathbf{J}}^T\tilde{\mathrm{f}} = \hat{\mathrm{g}}$, where $r$ is equal to the number of zero components of $\mathbf{J}\mathrm{a}_0$. The following two possibilities arise:

*Case 1* ($r = m - 1$): In this case only $m - 1$ components of $\mathbf{J}\mathrm{a}_0$ are zero. Since the vector equation $\hat{\mathbf{J}}^T\tilde{\mathrm{f}} = \hat{\mathrm{g}}$ is consistent and the rank of the $m \times (m-1)$ matrix $\hat{\mathbf{J}}$ is $m - 1$, it follows that there exists a unique solution given by

$$\tilde{\mathrm{f}} = (\hat{\mathbf{J}}\hat{\mathbf{J}}^T)^{-1}\hat{\mathbf{J}}\hat{\mathrm{g}} \tag{4.29}$$

where $\tilde{\mathrm{f}}$ is an $(m-1) \times 1$ vector whose components correspond to those components of f with $[\mathbf{J}\mathrm{a}_0]_0 = 0$.

*Case 2* ($r > m-1$): This case arises when $\mathbf{h}_q$ is orthogonal to more than $m-1$ rows of $\mathbf{J}$. Since $r > m-1$ and the rank of $\hat{\mathbf{J}}^T$ is $m-1$, the set of $m$ consistent equations in $r$ unknowns $\hat{\mathbf{J}}^T\tilde{\mathbf{f}} = \hat{\mathbf{g}}$ will have an infinity of solutions. By utilizing Theorem 2, the optimal $m$ constraints problem may be reduced to an $m-1$ costraint problem.

In summary, for a system of $m$ linear equations in $n$ unknowns, finding the optimal solution requires the computation of $N$ inner products of the form $\mathbf{g}^T\mathbf{h}_i$. The number $N$ is bounded from above by $\begin{pmatrix} n \\ m-1 \end{pmatrix}$. For moderate values of the parameters $m$ and $n$, the upper bound will be small enough to obtain a solution in an efficient manner. In fact, in our system, $m = 3$ and $n = 4$, an optimal solution can be obtained in at most six iterations.

As an example, when estimating a load of 10 $kg$, at static equilibrium, the force was measured, in Newtons, to be

$$\mathbf{f}^T = [203.45 \quad 194.23 \quad 105.42 \quad 126.47], \tag{4.30}$$

and the Jacobian matrix, expressed in units of $m$, was calculated, as explained in Chapter 2:

$$\mathbf{J} = \begin{bmatrix} -4.8666 & -2.9880 & 2.3246 \\ 4.9055 & -3.0118 & -2.2969 \\ 4.8876 & 3.0009 & 2.2584 \\ -4.2288 & 7.0999 & -2.0452 \end{bmatrix} \tag{4.31}$$

From the above, the torque vector is found to be

$$\bar{\tau}^T = [24.49 \quad 21.21 \quad 13.23] \quad Nm \tag{4.32}$$

Having $\bar{\tau}$, the optimal $\infty$_norm force vector can be calculated using the above technique:

$$\tilde{\mathbf{f}}_\infty^T = [-3.50 \quad -3.89 \quad 3.89 \quad -1.78] \tag{4.33}$$

Moreover, the optimal 2_norm force vector (in Hilbert space) can be found from (4.2):

$$\tilde{\mathbf{f}}_2^T = [-1.72 \quad -0.54 \quad 4.21 \quad 0.26] \tag{4.34}$$

It must be noted that that the kernel of $\mathbf{J}$,

$$\mathbf{n} = [0.63 \quad 0.60 \quad 0.31 \quad 0.39],$$

may be added to the both solutions without changing the output torque.

Comparing the two solutions, one will notice that the 2_norm solution has the least sum of the squares of the components, although, any individual component of the solutionmayhave a very high magnitude. While in the $\infty$_norm solution, the magnitudes og the components are as close as possible, therefore, the external force is compensated by the actuators as evenly as possible.

# Chapter 5 Conclusion

Starting from its constituents, the parallel shoulder was introduced in chapter 2. In particular, we began by describing the internal structure of
small **ASI** hydraulic actuators. These actuators have been used because of their high torque to mass ratios and extended force bandwidth. Moreover, their force to torque characteristics can be linearized [8]. Then the architecture of the shoulder was synthesized. Due to its parallel nature and actuator redundancy, it is free of singularities, free from backlash, and has good dynamic properties. At the end, the derivation of the kinematic relationships was reviewed [14].

Chapter 3 focused on the design and implementation of a controller for the shoulder using the relationships derived in chapter 2. This controller performs two functions: balances a slowly varying external force exerted on the endeffector, and estimates its magnitude. The structure of the controller consists of two parts, a damper and a coordinator. The former balances the force in the four actuators which result in restoring the static equilibrium. The latter ensures that this process takes place smoothly by coordinating the operation of the actuators.

The control functions are carried out in two steps. To avoid dealing with the nonlinearities introduced by the dynamics of the system, in the first step, the motion is damped to rest. Once in static equilibrium, the estimation function is performed. Because of the presence of the bias in measurements of the force, the bias vector must be estimated first. Having determined the bias, the external force, or the mass of the load in our case, can be easily calculated. Results of the experiments indicate an error of 10% in estimating the mass of a load using this method.

Chapter 4 was concerned with the optimization of the force vector. Since the mapping from actuator forces to the joint torque produces an overdetermined lin-

ear system of equations, there are infinite solutions for the vector of actuator forces for a given output torque. We have considered two of these solutions which yield two different optimal solutions in the form of minimum-norm vectors of forces. The first solution is a least square solution obtained by applying the generalized inverse of the transpose of the Jacobian matrix. The second minimum-norm vector was found in $l_\infty$ using the theory of the dual Banach Spaces.

The minimum $\infty$-norm solution was found using an algorithmic procedure. In this method, firstly the dual associated to the problem at hand is solved as specified by the duality theorems from functional analysis. Then the optimal solution is generated by using the alignment property. The speed of convergence depends on the size of the Jacobian matrix. For our system of 4 equations in 3 unknowns, this method requires 6 computations of inner products. Therefore, calculating the $\infty$-norm solution is even faster than finding the 2-norm solution.

These two methods were implemented and the results were presented. Comparing the two solutions, it becomes evident that the 2_norm solution minimizes the sum of the squares of the components, although, any individual component of the solution may have a very high magnitude. While in the $\infty$_norm solution, the largest magnitude is minimized and the magnitudes of the components are as close as possible, therefore, the external force is compensated by the actuators as evenly as possible.

## References


[1] An, C., Atkeson, C. G.and Hollerbach, J. M., "Model based control of a manipulator", *Cambridge Massachusetts: The MIT Press*, 1988.

[2] Asada, H. and Cro Granito, J. A., "Kinematic and static characterization of wrist joints and their optimal design", *Proc. IEEE Int. Conf. on Robotics and Automation*, pp. 244-250, 1985.

[3] Asada, H., and Ro, I. H., "A Linkage Design for Direct-Drive Robot Arms", *ASME J. of Mech., Trans., and Automation in Design*, Vol. 107, pp. 536-540, 1985.

[4] Asada, H. and Youcef-Toumi, K., "Analusis and design of direct-drive robo arms", *ASME j. dynamic Systems, Measurement, and Control*, vol. 106, pp. 225-230, 1984.

[5] Becker, M., "Design and kinematic modelling of a parallel redundant wrist", Engineer's Thesis, Institute B for Mechanics, Technical University of Munich, 1993.

[6] Becker, M., Hayward, V., Ranjbaran, F.and Anjeles, J., "The kinematics of a parallel wrist with actuation redundancy", To be presented at the Fifth Int. Symp. on Robotics and Manufacturing, ISRAM'94, Aug. 14-18, Hawaii, 1994.

[7] Boulet, B., "Modelling and control of a robotic joint with in-parallel redundant actuators", Master thesis, McGill University, Montreal, Quebec, Canada, 1992.

[8] Boulet, B., Daneshmend, L. K., Hayward, V., Nemri, C. 1993. System Identification and Modelling of a High Performance Hydraulic Actuator. *Experimental Robotics 2*, Chatila, R., Hirzinger, G. (Eds.), *Lecture Notes in Control and Information Sciences*, Springer Verlag.

[9] Cadzow, J. A., "A Finite Algorithm for the Minimum $l_\infty$ Solution to a System of Consistent Linear Equations", *SIAM J. Numer. Anal.*, vol. 10, no. 4, pp. 607-617, 1973.

[10] Gosselin, C. and Angeles, J, "The optimum kinematic design of a spherical three degree-of-freedom parallel manipulator", *ASME Advances in Design Automation: Robotics, Mechanisms, and Machine Systems*, DE-Vol. 10-2, pp. 111-115, 1987.

[11] Hayward, V., "An analysis of redundant manipulators from several viewpoints", *Robots with redundancy: design, sensing and control*, NATO Series, A. Bejczy (Ed.), Spring Verlag, 1989.

[12] Hayward, V., "Borrowing Some Design Ideas from Biological Manipulators to Design an Artificial One," in *Robots and Biological Systems, NATO Series*, P. Dario, P. Aebisher, and G. Sandini (eds.), Springer Verlag, In Press, 1991.

[13] Hayward, V. Design of a robot shoulder with with hydraulic actuator redundancy. *3rd Int. Symposium on Experimental Robotics*, Kyoto, Japan, 1993.

[14] Hayward, V. and Kurtz, R., L., "Kinematic Modelling of a parallel wrist mechanism with actuator redundancy", *LRA*, Vol. 4, pp 69-76, 1992.

[15] Hayward, V. and Kurtz, R., "Preliminary Study of Serial-Parallel Redundant Manipulator", *NASA Conference on Space Telerobotics*. JPL Publication 89-7, Vol II, Pasadena, CA. pp. 39–48, 1989.

[16] Hollerbach, J. M., and Suh, K. C., "Redundancy resolution of the manipulators through torque optimization", *IEEE J. of Robotics and Automation*, Vol. RA-3, No. 4, pp. 308-316, 1987.

[17] Hunt, K. H., "Structural kinematics of in-parallel-actuated robot-arms", *Proc. of the IEEE Micro Robots and Teleoperators Workshop: An Investigatio of Micromechanical Structures, Actuators, and Sensors*, Hyannis, Massachusetts, Paper 25/1-3, 1983.

[18] Inoue, H., Tsusaka, Y., Fukuizumi, T., "Parallel manipulator", *Robotics Research: The Third Intrnational Symposium*, pp. 321-327, 1986.

[19] Kerr, J. and Roth, B., "Analysis of multi-fingered hands", *The Int. J. of Robotics Research*, Vol. 4, No. 4, pp. 3-17, 1986a.

[20] Khatib, O. A., "Unified approach for motion and force control of robot manipulators: The operational space formulation", *IEEE J. Robotics and Automation*, Vol. RA-3, No. 1, 1987.

[21] Larsonneur, R., Arai, T, Jaya, Y. M. A six degree-of-freedom micro-manipulator using piezzoelectrically driven parallel link mechanism. Proc. 9th Conf. of the Robotic Society of Japan, Tsukuba, Japan, Nov. 27-29, 1991.

[22] Lee, K. and Shah, D. K., "Kinematic analysisof a three degrees of freedom in-parallel actuated manipulator", *Proc. IEEE Int. Conf. on Robotics and Automation*, pp. 345-350, 1987.

[23] Liégeois, A. Automatic supervisory control of the configuration and behavior of multi-body mechanisms. *IEEE Trans. on Syst., Man, and Cybernetics*. Vol. SMC 6(12), pp. 868–871, 1977.

[24] Luenberger, D. G., *Optimization by Vector Space Methods*. New-York: John Wiley & Sons, 1969.

[25] Luh, J. Y. S., and Gu, L. Y., "Indutrial robots with seven joints", *Proc. IEEE Int. Conf. on Robotis and Automation, St. Louis*, pp. 1010-1015, 1985.

[26] Luh, J. Y. S., Walker, M. W., Paul, R. P. C., "Resolved acceleration control of mechnical manipulators", *IEEE Transactions on Automatic Control*, Vol. AC-25, No. 3, 1980.

[27] Maciejewski, A. A., and Klein, C. A., "Obstacle avoidance for kinematically redundant manipulators in dynamically varying environments", *The Int. J. of Robotics Research*, Vol. 4, No. 3, pp. 109-117, 1985.

[28] Milenkovic, V., "New nonsingular wrist design", *Robots 11, The 17th Int. Symp. on Industrial Robots*, pp. 13-42, 1987.

[29] Nakamura, Y., "Dynamics of closed link robots with actuational redundancy", *Proc. of the Second Int. Symp. on Robotics and Manufacturing: Research, Education, and Publications*, pp. 309-318, 1988.

[30] Paul, R. P., and Stevenson, C. N., "Kinematics of robot wrists", *Int. J. Robotics Research*, vol. 2, No. 1, pp. 31-38, 1983.

[31] Phillips, J., "Freedom in Machinery. Vol 1: Introducing screw theory", Cambridge University Press, 1984.

[32] Phillips, J., "Freedom in Machinery. Vol 2: Screw theory exemplified", Cambridge University Press, 1990.

[33] Slotine, J. J. E., "The robust control of robot manipulators", *The Int. J. of Roborics Research*, Vol. 4, No. 2, 1985.

[34] Spring, K. W., "Euler Parameters and the Use of Quaternions Algebra in the Manipulation of Finite Rotations: A Review", *Mechanisms and Machine Theory*. 1986. pp. 365–373, Vol. 21, No. 5, 1986.

[35] Youcef-Toumi, K., "Analysis of dynmically decoupled mechnisms", *Proc. of the Second International Symposium on Robotics and Manufacturing: Research, Education, and Publications*, pp. 331-340, 1988.